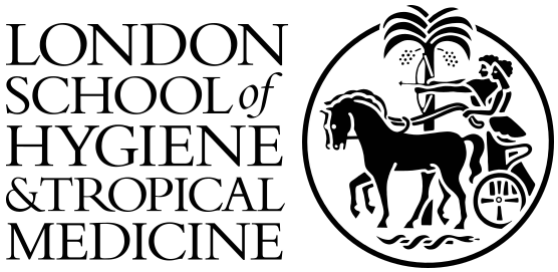

Title/Running Title: Pharmacokinetics and pharmacodynamics of the nitroimidazole DNDI-0690 in mouse models of cutaneous leishmaniasis

Byline: Gert-Jan Wijnant[1], Simon L. Croft[1], Raul de la Flor[2], Mo Alavijeh[2], Vanessa Yardley[1], Stéphanie Braillard[3], Charles Mowbray[3], Katrien Van Bocxlaer[1, 4]*

Affiliations:

[1] London School of Hygiene & Tropical Medicine, Faculty of Infectious and Tropical Diseases, Keppel Street, London WC1E 7HT, UK

[2] Pharmidex Pharmaceutical Services Ltd, 14 Hanover Street, London W1S 1YH, UK

[3] Drugs for Neglected Disease *initiative* (DND*i*), Chemin Louis Dunant 15, 1202 Geneva, Switzerland

[4] York Biomedical Research Institute, Department of Biology, University of York, York, YO10 5DD, UK

***Corresponding author**: Katrien Van Bocxlaer, York Biomedical Research Institute, Department of Biology, University of York, York, YO10 5DD, United Kingdom, katrien.vanbocxlaer@york.ac.uk, phone: 01904328855

Abstract:

The nitroimidazole DNDI-0690 is a clinical drug candidate for visceral leishmaniasis (VL) that also shows potent *in vitro* and *in vivo* activity against cutaneous leishmaniasis (CL). To support further development of this compound into a patient-friendly oral or topical formulation for CL, we investigated the free drug exposure at the dermal site of infection and subsequent

elimination of the causative *Leishmania* pathogen. This study evaluates the pharmacokinetics (PK) and pharmacodynamics (PD) of DNDI-0690 in mouse models of CL. Skin microdialysis and Franz diffusion cell permeation studies revealed that DNDI-0690 permeated poorly (< 1 %) into the skin lesion upon topical drug application (0.063 % W/V, 30 µl). In contrast, a single oral dose of 50 mg/kg resulted in the rapid and near-complete distribution of protein-unbound DNDI-0690 from the plasma into the infected dermis ($fAUC_{0\text{-}6h,\ tissue}$ / $fAUC_{0\text{-}6h\ blood}$ > 80 %). Based on *in vivo* bioluminescence imaging, two doses of 50 mg/kg DNDI-0690 were sufficient to reduce *L. mexicana* parasite load by 100-fold, while 6 such doses were needed to achieve similar killing of *L. major*; this was confirmed by quantitative PCR. The combination of rapid accumulation and potent activity in the *Leishmania*-infected dermis indicates the potential of DNDI-0690 as a novel oral treatment for CL.

Keywords: cutaneous leishmaniasis, drug development, microdialysis, skin pharmacokinetics, rate of kill

42 **Introduction**

43

44 Leishmaniasis is a poverty-associated infectious disease that has two main forms: visceral
45 leishmaniasis (VL) and cutaneous leishmaniasis (CL). While VL is almost invariably fatal if left
46 untreated, CL is not life-threatening but causes disfiguring skin lesions associated with severe
47 social stigma and psychological morbidity (1). The different types of CL have a wide geographic
48 distribution and vary in causative *Leishmania* parasite species, which are transmitted to humans
49 by infected female sand-flies. In the Middle-East, "Old World" *L. major* and *L. tropica* CL
50 commonly present as local papules, nodules or ulcers that are mostly self-limiting, but often
51 leave lifelong scars on the exposed skin areas. After healing, *L. tropica* CL can relapse into a
52 persisting, chronic form called leishmaniasis recidivans. In Central and South America, "New
53 World" parasite species of the *Leishmania* subgenus, such as L. *mexicana,* generally cause mild
54 forms of CL, while more complicated forms involving the mucous membranes of nose, throat
55 and mouth are observed in patients infected with the *Viannia* subgenus, for example *L.*
56 *braziliensis* (2, 3). An additional cutaneous manifestation is post-kala azar dermal leishmaniasis
57 (PKDL), a cutaneous sequela that can occur following the resolution of VL caused by *L.*
58 *donovani*, characterised by widespread macular or papular lesions (3, 4). Worldwide, around
59 0.7 to 1.2 million new cases of CL occur every year and around 1 billion people are at risk,
60 mostly those living in resource-poor environments (5). At present, treatment of CL is based on
61 four drugs: pentavalent antimonials, miltefosine, amphotericin B and paromomycin. All of these
62 have well-documented limitations of effectiveness, toxicity, cost or route of administration (6,
63 7). The Drugs for Neglected Diseases *initiative* (DND*i*), a non-profit drug development
64 partnership, has a strategy to deliver much-needed new drugs for CL. DND*i* defines the optimal

Target Product Profile (TPP) of a new chemical entity for CL as follows: (i) activity against all species of *Leishmania* causing CL (> 15), (ii) minimum 95% clinical efficacy and minimal scarring after accelerated healing of the skin lesions, (iii) oral or topical formulation for a maximum of 7 or 14 days, respectively (iv) well-tolerated and safe in pregnancy and (v) cost under $5 per course (8). Whilst topical formulations hold potential for the treatment of simple, self-healing lesions, oral drugs could be used for cases with a higher risk of parasite dissemination; both routes of administration avoid the need for painful drug injections that are currently common (9).

Nitroimidazoles are a medically important class of antimicrobial agents with a broad spectrum of activity, including against protozoan parasites such as *Trichomonas vaginalis*, *Trypanosoma cruzi* and *Giardia* (10). The prototype molecule for this class, metronidazole, was discovered in the 1950s, and in recent years there has been a renewed interest in the therapeutic potential of nitroimidazoles, especially as novel antitubercular agents (11). Indeed, successful drug development efforts have resulted in the regulatory approval of delamanid (OPC-67683) for the treatment of multi-drug resistant tuberculosis (TB) by the European Medicines Agency (EMA) (12), while another bicyclic nitroimidazole compound, pretomanid (PA-824), is currently under investigation in Phase III clinical trials (13). In 2010, DND*i* was granted access to a selected library of nitroimidazoles owned by the TB Alliance to speed up the development of novel therapies for neglected tropical diseases, including leishmaniasis. The antileishmanial activity of the nitroimidazooxazine DNDI-0690 (Figure 1) was first discovered in 2015; it is a structural analogue of DNDI-VL-2098 (14), a promising oral drug candidate for VL (15, 16) that was discontinued from further development due to toxicity issues identified during nonclinical CTA-enabling studies (6). Given its superior safety profile, potent *in vitro* activity (EC_{50} = 0.17 µM)

88 and excellent *in vivo* efficacy (> 99 % at 12.5 mg/kg p.o. twice a day in hamster models of VL)
89 (17, 18), the decision was made in 2018 to progress DNDI-0690 into in Phase 1 clinical trials for
90 VL. Furthermore, DNDI-0690 demonstrated excellent *in vitro* activity against three Old and
91 three New World cutaneous *Leishmania* strains (EC_{50} < 5 µM). In a mouse model of *L. major* CL,
92 oral DNDI-0690 exerted a linear dose-response effect (ED_{50} = 5 mg/kg, ED_{90} = 21 mg/kg,
93 maximal efficacy > 95 % for 50 mg/kg), while topical solutions applied directly to the skin lesion
94 were < 50 % active (19).

95 With the clinical evaluation of DNDI-0690 for VL underway, important questions about the
96 suitability, including appropriate PK and PD, of this nitroimidazole compound in the treatment
97 of CL remain. The PK and PD properties required of drug to cure the two forms of leishmaniasis
98 are not the same, due to (i) the different sites of infection that is the target for drug delivery
99 (liver, spleen and bone-marrow *versus* dermal skin layers), (ii) possible differences in drug
100 susceptibility between the causative parasites (*L. donovani* and *L. infantum* versus *L. major, L.*
101 *mexicana* and other dermatropic *Leishmania* species) (20) and (iii) the potential impact of
102 pathology on drug distribution. The aim of this study was to evaluate the PK and PD parameters
103 of DNDI-0690 as part of efforts to develop much-needed new oral or topical drugs to treat CL.
104 We therefore, determined the following properties of DNDI-0690: (i) *in vitro* drug disposition in
105 skin upon topical dosing (Franz diffusion cells), (ii) *in vitro* protein-binding (BCA protein assay)
106 and protein-binding corrected 50 % active drug concentrations against different CL-causing
107 *Leishmania* species (fEC_{50}), (iii) *in vivo* protein-free (e.g. pharmacologically active) drug exposure
108 at the dermal site of infection (microdialysis) and (iv) *in vivo* time-kill kinetics of *L. major* and *L.*
109 *mexicana* (bioluminescent parasite imaging).

110

Results

In vitro topical drug penetration

First, we evaluated topical drug penetration of DNDI-0690 into mouse skin *in vitro* using Franz diffusion cell permeation assays to investigate why the topical application of DNDI-0690 led to limited anti-leishmanial activity in murine models of CL (19). Table 1 shows skin distribution of topical DNDI-0690 into healthy and diseased but visibly intact skin (average nodule diameter 4.10 ± 0.72 mm) harvested from *L. major*–infected BALB/c mice. Six hours after application of a solution of DNDI-0690 saturated in ethanol:propylene glycol (EtOH:PG) (0.063 % W/V), around 99.5 % of the drug remained on the skin surface. Only a limited amount of drug (0.07-0.34 %) penetrated into the deeper layers of the (epi)dermis and 0.15-0.03 % passed through the skin, indicating poor dermal retention. There was no significant difference in drug quantity found in the different layers of the skin between *L. major*-infected and uninfected skin ($p > 0.05$).

In vitro anti-leishmanial drug activity corrected for protein binding

Second, *in vitro* 50 % effective concentrations (EC_{50}) against *Leishmania* corrected for protein-binding (fEC_{50}) were calculated. This was done to enable comparison between *in vitro* PD measures (EC_{50} value based on total drug concentrations in the drug assay medium) and *in vivo* PK parameters obtained by microdialysis (non-protein bound drug concentrations). Therefore, protein-binding in the *in vitro* assay medium (RPMI containing 10 % heat-inactivated foetal calf serum, HiFCS) was estimated using a rapid equilibrium method. Drug-protein binding in the medium was moderate: 45.8 % at 0.2 µM and 53.1 % at 1 µM DNDI-0690. The mean % binding

for DNDI-0690 (49.6 %) was used to determine fEC$_{50}$, based on previously obtained EC$_{50}$ values (19) and described in Table 2.

***In vivo* skin pharmacokinetics**

Third, we studied the *in vivo* skin PK of DNDI-0690 in the *L. major*-BALB/c mouse model using microdialysis. After administration of either a single oral (50 mg/kg) or topical (30 µl 0.064 % w/v) dose of DNDI-0690 to the infected mice, free drug concentrations in the infected dermis (target site), the uninfected dermis (off-target site) and plasma (systemic circulation) were determined (Figure 2). After oral dosing at 50 mg/kg, DNDI-0690 showed a gastrointestinal absorption delay of 2.5 hours before reaching an fC$_{max}$ of 275.4 ± 37.9 nM in the blood. Systemic drug concentrations remained stable in the following 3.5 hours, indicating a plasma half-life (T$_{1/2}$) > 4 hours. Distribution volume (Vd) and elimination rate constant (Ke) values could not be estimated because no significant clearance of DNDI-0690 from plasma occurred within 6 hours of oral drug administration (t$_{last}$). The concentration of unbound DNDI-0690 in plasma was similar to unbound drug concentrations in infected and uninfected skin tissue and followed a comparable trend. Drug penetration from blood into skin tissue was high (fAUC$_{0\text{-}6h,\ tissue}$ / $_f$AUC$_{0\text{-}6h\ blood}$ > 80 %) and maximal after 6 hours of oral dosing. However, DNDI-0690 concentrations and overall drug distribution to cutaneous tissues were increased in uninfected in comparison to infected skin (C$_{max}$ = 365.3 ± 47.1 nM *versus* 263.7 ± 28.0 nM; AUC$_{0\text{-}6h,\ tissue}$ / AUC$_{0\text{-}6h\ blood}$ = 136.7 % v*ersus* 82.1 %, respectively). In contrast, after topical application of 50 µl DNDI-0690 saturated solution to the lesion, no drug was detected in the infected dermis within the following 6 hours. All results shown are corrected for *in vitro* relative recovery (RR) of DNDI-

0690 from the microdialysis probe. The RR was 18.6 ± 2.3 % and independent of concentration under *in vitro* experimental conditions mimicking those *in vivo*.

***In vivo* antileishmanial pharmacodynamics**

Fourth, the time-kill kinetics of DNDI-0690 were characterised in two BALB/c mouse models of CL using bioluminescent *L. major* and *L. mexicana* parasites. Topical activity of DNDI-0690 was not evaluated due to poor skin permeation and low efficacy when administered via this route. After oral dosing of DNDI-0690 (50 mg/kg once daily for ten days), rapid and complete clearance of *L. major* and *L. mexicana* from the infected mice was observed (Figures 3 and 4, respectively). A 10-, 100- and close to 1000-fold reduction in *L. major* parasite load (relative to organism burden in untreated mice at the same time-point) was observed by days 2, 6 and 10, respectively. The maximal killing of *L. major* (99.5 %) was achieved 24 hours after the 10th and final dose of DNDI-0690 (day 10). At this point, the efficacy of DNDI-0690 was comparable to that of the positive control drug intravenous liposomal amphotericin B (LAmB, 99.7%) in this model. An identical regimen of once daily 50 mg/kg DNDI-0690 resulted in a 100-fold reduction in *L. mexicana* parasite burden by day 2. After two oral doses, the bioluminescent signal in the DNDI-0690 treated group was indistinguishable from that of the mice infected with wild-type, not-bioluminescent parasites. The activity of DNDI-0690 against *L. mexicana* was maximal (99.4 %) and higher than that of LAmB (89.0%) at the end of treatment (day 10). Quantitative PCR was used to confirm the > 99 % reductions in parasite load for *L. major*- and *L. mexicana*-infected mice treated with oral DNDI-0690 compared to untreated controls (Figures 3 (C) and 4 (C), respectively).

177 **Discussion**

178 We have demonstrated the potential of DNDI-0690 as a novel treatment for CL by the oral
179 route and the limited potential for its topical application. After oral administration at 50 mg/kg,
180 DNDI-0690 is rapidly absorbed into the bloodstream and completely distributed to the skin,
181 reaching near-maximal drug exposure at the site of action within 3 hours. At the dermal
182 infection site, fC_{max} was lower (0.26 ± 0.03 µM) than fEC_{50} values for all tested *Leishmania*
183 species (0.4 - 12 µM), indicating multiple doses could be needed to allow drug distribution to
184 infected tissues and achieve cure. *In vivo* time-kill studies confirmed this was the case; in order
185 to obtain a 100-fold reduction in lesion parasite load, 2 doses of 50 mg/kg were needed to clear
186 *L. mexicana* (fEC_{50} = 0.96 µM) versus 6 doses for *L. major* (fEC_{50} = 3.15 µM). In both these
187 bioluminescent *Leishmania* parasite CL mouse models, oral DNDI-0690 was as efficacious as the
188 intravenous anti-leishmanial drug LAmB at the end of the 10-day treatment (> 99%). In
189 contrast, topical administration of DNDI-0690 as a single application to the skin lesion did not
190 result in measurable drug levels in the infected dermis. This may explain the low efficacy (< 50
191 % reduction of lesion size and parasite burden determined by qPCR) of treatment via this route
192 seen in earlier studies (19). These poor *in vivo* drug penetration kinetics, determined by skin
193 microdialysis, were successfully predicted by *in vitro* Franz diffusion cell assays, which revealed
194 the inability of DNDI-0690 to permeate the epidermis (> 99 % drug was recovered from the skin
195 surface). Such assays therefore save time and resources for the design and development of new
196 topical formulations to treat simple CL (21).

197 To the best of our knowledge, this is the first time that skin microdialysis has been used to
198 evaluate PK in *Leishmania*-infected mouse skin. The main technical advantage of this method
199 for *in vivo* CL drug research is that it continuously measures protein-free (and, thus,

pharmacologically active) drug concentrations directly in the dermal interstitial fluid surrounding the parasitized macrophages (22). Voelkner and colleagues employed a similar approach to evaluating the proposed anti-leishmanial drug pyrazinamide, although this experiment was performed in healthy rats (23).

Interestingly, we observed differences in the PK of oral DNDI-0690 in *Leishmania*-infected and uninfected skin. Inflammation at the infection site in CL affects local drug distribution after intravenous administration of different formulations of amphotericin B (24, 25), as well as of topical drugs (26). Unbound DNDI-0690 concentrations in the dermal interstitial fluid could be lower in diseased than healthy skin, because while higher absolute amounts of drug may reach the skin tissue from the bloodstream (increased vascular permeability, vasodilation) (25), more drug could be bound to inflammatory proteins or engulfed by macrophages in the dermis. As neither protein-bound nor intracellular drug fractions are measured by microdialysis (27), this could explain the ultimately lower extracellular exposure of DNDI-0690 at the site of infection compared to uninfected counterparts. This finding illustrates the impact of the CL pathology on local drug distribution in the skin. Differences between amphotericin B and DNDI-0690 PK results could be related to the different sampling methodologies (skin necropsies and microdialysis, respectively).

A limitation of this work is the single, high dose of oral DNDI-0690 (50 mg/kg) that was used during the PK and PD experiments. Further dose fractionation studies are required to identify the PK/PD driver of efficacy in CL (28). Combined with extended PK studies in mice and man (different dose levels and, time points > 6 hours), available data on the susceptibility of six parasite species and strains to DNDI-0690 can be used to set a robust PK/PD target estimate to inform the design of optimal clinical dosing regimens.

223 In conclusion, the rapid oral absorption and potent activity of DNDI-0690 in skin lesions caused
224 by *L. major* and *L. mexicana* support further development of this preclinical drug candidate as a
225 new oral treatment for CL.

226

227

228 **Materials and methods**

229 **Drugs and reagents**. Oral DNDI-0690 was formulated in polyethylene glycol 400 (PEG400). The
230 suspension was prepared in glass vials containing glass beads and sonicated (CamLab,
231 Cambridge, UK) for 15 minutes before use. The dose levels and dosing frequency chosen were
232 based on efficacy observed against VL (18) and CL (20). Topical DNDI-0690 was formulated as a
233 saturated solution in propylene glycol-ethanol (PG-EOH, 1:1) to maximize permeation through
234 the skin. The preparation was as follows. Excess of drug compound was added to a glass vial
235 together with 1mL of PG-EtOH (1:1) and a magnetic stirrer. The vial was covered with
236 aluminium foil and left at 34°C for 24 hours. An aliquot of this suspension was transferred to a
237 vial and centrifuged for 15 min at 18,407 x *g* and 34°C after which the supernatant was
238 transferred to a clean vial and stored at 4°C until drug administration. LC-MS/MS analysis
239 confirmed the concentration of DNDI-0690 in this topical vehicle to be 0.063 % (W/V). Ringers
240 solution was prepared at full strength (Sigma Aldrich) dissolved in 500 ml purified water) and
241 autoclaved before use.

242 **Parasite maintenance, animals and ethical statement.** The bioluminescent strains *Ppy RE9H+L.*
243 *major* Friedlin (MHOM/IL/81/Friedlin) and *Ppy RE9H+L. mexicana* M379 (MNYC/BZ/62/M379)
244 were kindly provided by Elmarie Myburgh and Jeremy Mottram (University of York, UK). *L.*
245 *major* JISH WT (MHOM/SA/85/JISH118), *Ppy RE9H+L. major* Friedlin and, *Ppy RE9H+L. mexicana*
246 M379 were maintained in Schneider's medium supplemented with 10% heat-inactivated foetal
247 calf serum (HiFCS) and passaged weekly (1:10). Female BALB/c mice (age 6-8 weeks) were
248 purchased from Charles River (Margate, UK) and left to acclimatise for 5 days upon arrival. One
249 day prior to infection, the rump above the tail was shaven using electric clippers. Twenty-four
250 hours later, low-passage late-stationary phase promastigote cultures were centrifuged at 900 x

g for 10 min at 4°C, counted using an improved Neubauer haemocytometer and re-suspended to 2 x 10^8 promastigotes per ml. Mice were subcutaneously injected in the rump with 200 µl of the suspension and randomly grouped (n=3-5). The mice were housed in a controlled environment of 55% relative humidity and 26°C and provided with tap water and a standard laboratory diet. All *in vivo* experiments were carried out under license (X20014A54) at the London School of Hygiene and Tropical Medicine (LSHTM) after discussion with the Named Veterinarian Surgeon and according to UK Home Office regulations.

Bioanalysis of DNDI-0690 (LC-MS/MS). All samples were analyzed using a Shimadzu Nexera X2 UHPLC/Shimadzu LCMS 860 at Pharmidex Pharmaceutical Services Ltd (Hatfield, UK). A mobile phase (0.4 ml/min) of water-0.1%formic (channel A) and acetonitrile-0.1%formic acid (channel B) was used to elute the sample compound from a Kinetex 5-µm XB-C_{18} column (2.1 mm by 50 mm at 50 °C; Phenomenex, UK). The mobile phase composition was initially 2% B, programmed to increase linearly to 95% B at 1.1 minutes after injection. After 0.7 minutes at 95 % B, the composition was returned to its initial 2% B at 1.8 minutes post-injection. DNDI-0690 was detected by monitoring the transition of the parent molecule (mass-to-charge ratio (m/z) 370) to the fragment resulting from electrospray ionization (m/z 198.2). Analyte concentrations were quantified against calibration standards prepared in matched control matrices, with aliquots of samples, blanks and standards being injected at 5 µl. Lower limit of quantifications ranged between 0.5ng/ml and 50ng/ml for the microdialysis and skin extraction samples, respectively (Supplemental material 1).

***In vitro* drug binding.** The *in vitro* binding of the drug compounds to skin components was measured using the Rapid Equilibrium Dialysis single-use Device (Pierce Red Device, ThermoScientific). A 20 mM solution of DNDI-0690 in DMSO was used to spike RPMI-1640

medium supplemented with 10% HiFCS to a final concentration of 0.2 and 1 µM of DNDI-0690. Three hundred µL of the DNDI-0690 containing medium was transferred to the sample chamber and 550 µL of Ringers solution was added to the buffer chamber. This was done in triplicate for each DNDI-0690 concentration. The RED device was left to incubate in an orbital shaking incubator (200 rpm) at 34 °C for 4 hours. From each chamber, 50 µl aliquots were collected and matrix matched after which 2 volumes of ice cold ACN were added. After another 20 minutes, 100 µL of each mixture was centrifuged for 15 minutes at 21,130 x g at 4°C. The supernatants were assayed for the parent drug by LC-MS/MS.

Franz diffusion cell permeation and drug disposition. Female BALB/c mice (n=5) were injected subcutaneously with 4 x 10^7 *L. major* promastigotes above the tail. In time, a nodule developed at the injection site and when this reached 4 to 5mm the mice were sacrificed using CO_2. Two circular skin discs (approximately 15 mm diameter) were obtained per donor mouse; one containing the leishmaniasis nodule (average ± sd) that was collected from the lower dorsal area above the tail and another disc of unaffected skin that was collected from the area higher up the back of the mouse. Fat and muscle tissue were carefully removed using forceps and the skin was gently stretched on Whatman filter paper. The skin was placed between the greased donor and receptor compartment of the Franz cell with a narrow diameter (5 mm). PBS was sonicated for 30 minutes and added to the receptor compartment together with a small magnetic stirrer. The Franz cells were placed on the magnetic stirrer plate (800 rpm) in a warm water bath until the skin temperature reached a steady 34°C. Next, the DNDI-0690 saturated solution (30µL of 0.064% (W/V) DNDI-0690 in PG: EtOH (1:1)) was applied to the skin and 100 µl of receptor solution was replaced with fresh PBS at regular time intervals over a period of 6 hours and analysed by LC-MS/MS. At the end of the experiment, the cells were dismantled and

297 the donor chambers of the Franz cells were washed with 1 ml of acetonitrile: water solution
298 (ACN: H_2O (1:1)). Any drug remaining on the skin surface was removed using a clean dry cotton
299 swab. The amount of drug in the washing liquid and the cotton swab was quantified using LC-
300 MS/MS. To extract DNDI-0690 from the skin, the skin disc was homogenised in 1 ml of PBS as
301 described above. 100 µL of this homogenate was protein precipitated using 300 µL of ice-cold
302 ACN (100 %) and, centrifuged at 13,000 rpm for 30 mins at 4°C. An aliquot of the supernatant
303 was diluted with an equal volume of water and stored for analysis by LC-MS/MS at -80°C.
304 Together the amount of drug recovered from the skin surface, extracted from the skin and
305 permeated through the skin was satisfactory when ranging from 70-110%.

306 **Microdialysis system.** MAB 1.2.4. Cu probes (Microbiotech, Sweden) with a 6kDa cut-off
307 cuprophane membrane were used *in vitro* for recovery determination and *in vivo* for
308 microdialysis. The cuprophane membrane of this concentric probe is 2 mm long and has an
309 outer membrane diameter of 0.2 mm; inlet and outlet tubing consisted of fluorinated ethylene
310 propylene (FEP) with lengths of 25 and 50 cm, respectively. A syringe pump (11 plus model 70-
311 2208, Harvard Apparatus, USA) was used to circulate the perfusate (Ringers solution) at a flow
312 rate of 2 µl/minute. Dialysates were automatically collected in glass vials (Thermo Fisher, UK)
313 using a refrigerated fraction collector (MAB 85, Microbiotech, Sweden) at 30 minutes set
314 intervals. For accurate measurement of *in vivo* free drug concentrations at the dermal site of
315 action, raw microdialysis values were corrected for the loss of compound due to incomplete
316 equilibration between the sampling medium and the perfusate and/or sticking of the drug to
317 the outlet tubing of the microdialysis probe, expressed as the relative recovery value (22).
318 Recovery rates for the microdialysis equipment were determined *in vitro* as follows: three
319 probes were placed in a reservoir containing DNDI-0690 at concentrations of 30 or 120 ng/ml in

320 Ringers solution at 34 °C (mimicking *in vivo* skin temperature). The probes were perfused with
321 Ringers solution at a flow rate of 2 µl/minute and microdialysates were collected every 15
322 minutes. All samples were analysed using LC-MS/MS after the addition of 10 µl acetonitrile
323 (ACN) (1:3 ratio for 30 µl sample volume). Relative recovery (RR) was calculated as the ratio of
324 the analyte concentrations in the microdialysate over the analyte concentration in the reservoir
325 medium.

326 ***In vivo* microdialysis.** *L. major* JISH-infected BALB/c mice (n=6) with shaven rump and back
327 were anaesthetised with 1.6 g/kg urethane (IP). Two hundred µl Ringers physiological solution
328 was immediately administered via the neck scruff (SC) to prevent dehydration during long-term
329 (6-8 hour) anaesthesia. Mice were placed on a temperature-controlled heating pad (Peco
330 Services Ltd, Cumbria, UK) to maintain body temperature at 32 ± 2 °C. MAB 1.2.4. probes were
331 inserted in the following positions using a 22 G needle: the dermal skin layer of the CL lesion on
332 the rump, the dermal skin layer of the healthy control skin higher up on the back and the tail
333 vein (Figure 5). To equilibrate the system and allow the skin and tail vein to recover from the
334 probe insertion trauma, a stabilisation period of 30 minutes (23) of perfusion with Ringers
335 solution at a flow rate of 2 µl/min was included before collecting samples. At the start of the
336 pharmacokinetic experiment, half of the mice (n=3) received 50 mg/kg DNDI-0690 via oral
337 gavage. This dosage has been shown to significantly reduce the lesion size (20). The other three
338 mice received 30 µl of a 0.064 % (W/V) saturated solution (maximal driving force of 1) applied
339 topically to the skin lesion on the rump of the mice. Samples were collected every 30 minutes at
340 a flow rate of 2 µl/min. After the addition of 20 µl acetonitrile (1:3 ratio for 60 µl sample
341 volume) samples were stored at – 80 °C before analysis by LC-MS/MS. Temperature, breathing

pattern and behaviour of the anaesthetized mice were monitored constantly. At the end of the experiment, mice were culled by pentobarbital overdose.

Single-dose PK parameters were calculated by plotting the DNDI-0690 concentrations measured in the dialysate of the probe placed in the blood vene, the infected and uninfected skin over time. The *f*Cmax for each matrix (blood, infected and uninfected skin) is the highest drug concentration reached in each respective matrix throughout the experiment. $fAUC_{0-6h}$ values for the blood and infected and uninfected skin were calculated using GraphPad Prism, version 7.02. Data are presented as mean and standard error of the mean (SEM).

Rate-of-kill by *in vivo* bioluminescence imaging. Thirty-six female BALB/c mice were purchased and prepared for infection as described above. Fifteen mice were injected with 4 x 10^7 stationary phase luciferase-expressing *L. major* Friedlin (*Ppy RE9H+L. major* Friedlin*)* promastigotes, fifteen were injected with luciferase-expressing *L. mexicana* M379 (*Ppy RE9H+L. mexicana* M379*)* (23) and six were infected with *L. major* JISH WT parasites that do not express luciferase. Upon appearance, nodule diameters were measured in two directions daily. When the size progressed to 6.73 ± 1 mm for the *L. major* Friedlin-infected mice, they were allocated into groups of five with similar average nodule diameters ($p>0.5$, One-Way ANOVA) and treatment was initiated. For the *Ppy RE9H+L. mexicana* M379, no lesions developed and treatment was started when the bioluminescence signal reached 5.02 (± 3.27) x 10^6 radiance/second. Each experiment included an untreated control (n=5), baseline control (*L. major* JISH WT, n=3), positive control (AmBisome®, iv, 25mg/kg, QAD, n=5) and a DNDI-0690 group (50 mg/kg, po, QD, n=5). A topical administration group was not included due to previously observed inactivity. The bioluminescent signal was measured prior to administration of the first drug dose and every other day thereafter until the baseline signal was reached. Ten

minutes before acquiring the bioluminescent signal, mice were injected with 150 mg/kg luciferin (d-luciferin potassium salt, (Bertin Bioreagent), then anesthetized using 3 % (vol/vol) gaseous isoflurane and placed in an IVIS Lumina II system (Perkin Elmer). Images were acquired 10 minutes after luciferin injection using LivingImage v4.3. A circular region of interest (ROI) encompassing the nodular area on the rump was drawn to quantify bioluminescence expressed as radiance (photons/second/cm^2/sr). Background radiance was measured from mice infected with *L. major* JISH WT. Parasite burden in the skin was confirmed by DNA-based qPCR, as described earlier (24).

Statistical analysis. For the *in vitro* topical drug penetration experiment, differences between DNDI-0690 concentrations in healthy and infected skin were compared using student t-test (Prism v 7.02, Graphpad). To compare differences in qPCR parasite load in skin lesions, 1-way analysis of variance (ANOVA) followed by Dunnett's multiple-comparison test was performed. A *P* value of <0.05 was considered statistically significant.

Acknowledgements

DND*i* received financial support for this work from the following donors: Dutch Ministry of Foreign Affairs (DGIS), the Netherlands; Federal Ministry of Education and Research (BMBF) through KfW, Germany; World Health Organization – Special Programme for Research and Training in Tropical Diseases (WHO-TDR); and for its overall mission from Médecins sans Frontières, International; the Swiss Agency for Development and Cooperation (SDC), Switzerland; and UK aid, UK. KVB was funded by DND*i*. GJW has received funding from the European Horizon's 2020 Research and Innovation Programme as part of the EuroLeish.Net

387 Training Network under the Marie Sklodowska-Curie grant agreement number 642609. SLC and
388 VY were supported by Wellcome Trust Grant (104976).
389 The authors thank Dr. Elmarie Myburgh and Professor Jeremy Mottram (University of York) for
390 providing the bioluminescent *L. major* Friedlin and *L. mexicana* M379. We are grateful to
391 Professor Jennifer Linden (UCL Ear Institute), the BSF staff and Arturo Fernandez for the helpful
392 discussions.

References

1. Bailey F, Mondragon-Shem K, Haines LR, Olabi A, Alorfi A, Ruiz-Postigo JA, Alvar J, Hotez P, Adams ER, Velez ID, Al-Salem W, Eaton J, Acosta-Serrano A, Molyneux DH. 2019. Cutaneous leishmaniasis and co-morbid major depressive disorder: A systematic review with burden estimates. PLoS Negl Trop Dis 13:e0007092.
2. Alvar J, Arana B. 2018. Leishmaniasis - impact and therapeutic needs, p 3-23. *In* Rivas L, Gil C (ed), Drug Discovery for Leishmaniasis. The Royal Society of Chemistry, Croyden, UK.
3. Reithinger R, Dujardin JC, Louzir H, Pirmez C, Alexander B, Brooker S. 2007. Cutaneous leishmaniasis. Lancet Infectious Diseases 7:581-596.
4. Pijpers J, den Boer ML, Essink DR, Ritmeijer K. 2019. The safety and efficacy of miltefosine in the long-term treatment of post-kala-azar dermal leishmaniasis in South Asia – A review and meta-analysis. PLOS Neglected Tropical Diseases 13:e0007173.
5. WHO. 2016. Leishmaniasis in high-burden countries: an epidemiological update based on data reported in 2014 WHO Weekly epidemiological record 22:285-296.
6. Mowbray CE. 2018. Anti-leishmanial drug discovery: past, present and future perspectives, p 24-36. *In* Rivas L, Gil C (ed), Drug Discovery for Leishmaniasis. The Royal Society of Chemistry, Croyden, UK.
7. Croft SL, Olliaro P. 2011. Leishmaniasis chemotherapy-challenges and opportunities. Clinical Microbiology and Infection 17:1478-1483.
8. DND*i*. 2019. Target Product Profile for Cutaneous Leishmaniasis, *on* Drugs for Neglected Diseases *initiative*. https://www.dndi.org/diseases-projects/leishmaniasis/tpp-cl/. Accessed 21 February 2019.
9. Aronson N, Herwaldt BL, Libman M, Pearson R, Lopez-Velez R, Weina P, Carvalho E, Ephros M, Jeronimo S, Magill A. 2017. Diagnosis and Treatment of Leishmaniasis: Clinical Practice Guidelines by the Infectious Diseases Society of America (IDSA) and the American Society of Tropical Medicine and Hygiene (ASTMH). Am J Trop Med Hyg 96:24-45.
10. Ang CW, Jarrad AM, Cooper MA, Blaskovich MAT. 2017. Nitroimidazoles: Molecular Fireworks That Combat a Broad Spectrum of Infectious Diseases. J Med Chem 60:7636-7657.
11. Mukherjee T, Boshoff H. 2011. Nitroimidazoles for the treatment of TB: past, present and future. Future Med Chem 3:1427-54.
12. Ryan NJ, Lo JH. 2014. Delamanid: first global approval. Drugs 74:1041-5.
13. Medicine USNLo. 2019. A Phase 3 Study Assessing the Safety and Efficacy of Bedaquiline Plus PA-824 Plus Linezolid in Subjects With Drug Resistant Pulmonary Tuberculosis, *on* U.S. National Library of Medicine. https://clinicaltrials.gov/ct2/show/NCT02333799. Accessed 21 February 2019.
14. Thompson AM, O'Connor PD, Marshall AJ, Blaser A, Yardley V, Maes L, Gupta S, Launay D, Braillard S, Chatelain E, Wan B, Franzblau SG, Ma Z, Cooper CB, Denny WA. 2018. Development of (6 R)-2-Nitro-6-[4-(trifluoromethoxy)phenoxy]-6,7-dihydro-5 H-imidazo[2,1- b][1,3]oxazine (DNDI-8219): A New Lead for Visceral Leishmaniasis. J Med Chem 61:2329-2352.
15. Mukkavilli R, Pinjari J, Patel B, Sengottuvelan S, Mondal S, Gadekar A, Verma M, Patel J, Pothuri L, Chandrashekar G, Koiram P, Harisudhan T, Moinuddin A, Launay D, Vachharajani N, Ramanathan V, Martin D. 2014. In vitro metabolism, disposition, preclinical pharmacokinetics and prediction of human pharmacokinetics of DNDI-VL-2098, a potential oral treatment for Visceral Leishmaniasis. Eur J Pharm Sci 65:147-55.
16. Gupta S, Yardley V, Vishwakarma P, Shivahare R, Sharma B, Launay D, Martin D, Puri SK. 2015. Nitroimidazo-oxazole compound DNDI-VL-2098: an orally effective preclinical drug candidate for the treatment of visceral leishmaniasis. J Antimicrob Chemother 70:518-27.

17. Van den Kerkhof M, Mabille D, Chatelain E, Mowbray CE, Braillard S, Hendrickx S, Maes L, Caljon G. 2018. In vitro and in vivo pharmacodynamics of three novel antileishmanial lead series. Int J Parasitol Drugs Drug Resist 8:81-86.
18. DND*i*. 2019. Projects and Portfolio - DNDI-0690, *on* Drugs for Neglected Diseases *initiative*. https://www.dndi.org/diseases-projects/portfolio/dndi-0690/. Accessed 20-6-19.
19. Van Bocxlaer K, Caridha D, Black C, Vesely B, Leed S, Sciotti R, Wijnant G, Yardley V, Braillard S, Mowbray C, Ioset J, Croft S. 2019. Novel benzoxaborole, nitroimidazole and aminopyrazoles with activity against experimental cutaneous leishmaniasis. International Journal for Parasitology: Drugs and Drug Resistance.
20. Croft SL. 2017. Leishmania and other intracellular pathogens: selectivity, drug distribution and PK–PD: [BSP Autumn Symposium "Microbial protein targets: towards understanding and intervention", 14th–16th September 2016, University of Durham UK]. Parasitology doi:10.1017/S0031182017001664:1-11.
21. Van Bocxlaer K, Gaukel E, Hauser D, Park SH, Schock S, Yardley V, Randolph R, Plattner JJ, Merchant T, Croft SL, Jacobs RT, Wring SA. 2018. Topical Treatment for Cutaneous Leishmaniasis: Dermato-Pharmacokinetic Lead Optimization of Benzoxaboroles. Antimicrob Agents Chemother 62:e02419-17.
22. Mouton JW, Theuretzbacher U, Craig WA, Tulkens PM, Derendorf H, Cars O. 2008. Tissue concentrations: do we ever learn? Journal of Antimicrobial Chemotherapy 61:235-237.
23. Voelkner NMF, Voelkner A, Costa J, Sy SKB, Hermes J, Weitzel J, Morales S, Derendorf H. 2018. Dermal pharmacokinetics of pyrazinamide determined by microdialysis sampling in rats. International Journal of Antimicrobial Agents 51 190-196.
24. Wijnant GJ, Van Bocxlaer K, Yardley V, Harris A, Murdan S, Croft SL. 2018. Relation between Skin Pharmacokinetics and Efficacy in AmBisome Treatment of Murine Cutaneous Leishmaniasis. Antimicrobial Agents and Chemotherapy 62:e02009-17.
25. Wijnant GJ, Van Bocxlaer K, Fortes Francisco A, Yardley V, Harris A, Alavijeh M, Murdan S, Croft SL. 2018. Local Skin Inflammation in Cutaneous Leishmaniasis as a Source of Variable Pharmacokinetics and Therapeutic Efficacy of Liposomal Amphotericin B. Antimicrob Agents Chemother 62:e00631-18.
26. Van Bocxlaer K, Yardley V, Murdan S, Croft SL. 2016. Drug permeation and barrier damage in Leishmania-infected mouse skin. J Antimicrob Chemother 71:1578-85.
27. Groth L, Garcia Ortiz P, Benfeldt E. 2006. Microdialysis methodology for sampling in the skin, p 443-454. *In* Serup J, Jemec GBE, Grove GL (ed), Handbook of non-invasive methods and the skin, second edition ed. CRC/Taylor & Francis., Boca Raton.
28. Gumbo T, Angulo-Barturen I, Ferrer-Bazaga S. 2015. Pharmacokinetic-pharmacodynamic and dose-response relationships of antituberculosis drugs: recommendations and standards for industry and academia. J Infect Dis 211 Suppl 3:S96-s106.

Tables

Table 1. Disposition of topically applied DNDI-0690 in the skin of *L. major*-infected BALB/c mice using Franz diffusion cells. The total amount of DNDI-0690 per FDC recovered at the end of the experiment was considered 100%. The amounts of DNDI-0690 recovered from the different sites were expressed as a fraction of this amount. The table shows the average % (± SD), (infected n=5, uninfected n=3).

DNDI-0690 localisation	Uninfected skin	Infected skin	P-value (t-test)
On skin (DNDI-0690 in wash and cotton swab)	99.63 (± 0.39)	99.77 (± 0.19)	0.49
In skin (DNDI-0690 extracted from skin homogenate)	0.34 (± 0.39)	0.07 (± 0.07)	0.16
Through skin (DNDI-0690 in receptor fluid)	0.03 (± 0.05)	0.15 (± 0.15)	0.227

Table 2. Protein binding-corrected 50 % effective concentrations (*f*EC50) of DNDI-0690 against several cutaneous *Leishmania* species (n is the number of experiment repeats).

CL- causing *Leishmania* species	n	EC_{50} (µM)	fEC_{50} (µM)
L. major (MHOM/SA/85/JISH118)	1 2	4.56 7.94	2.28 3.97
L. tropica (MHOM/AF/2015/HTD7)	1 2	1.41 2.38	0.71 1.19
L. aethiopica (MHOM/ET/84/KH)	1 2	24.61 < 0.33	12.31 < 0.165
L. mexicana (MNYC/BZ/62/M379)	1 2	1.91 <1.11	0.96 <0.56
L. panamensis (MHOM/PA/67/BOYNTON)	1	0.77	0.39
L. amazonensis DsRed2	1	< 1.11	< 0.56

Figure legends

Figure 1. The chemical structure of DNDI-0690.

Figure 2. Skin PK of DNDI-0690 in the *L. major*-BALB/c mouse model of CL after oral (left - each mouse had 3 probes inserted: tail vein, healthy and lesion skin) and topical (right - each mouse had 1 probe inserted: lesion skin) drug administration. Data represent protein-free drug concentrations (average concentration (nM) ± SD (n=3)), corrected for probe recovery.

Figure 3. Anti-leishmanial efficacy of oral DNDI-0690 (50 mg/kg, once daily for 10 days) in an 'Old World' CL model (*L. major* Friedlin REH infection of BALB/c mouse). (A) shows the parasite load, as indicated by *in vivo* imaging of bioluminescent parasites in the infected rump skin over time. (B) shows the bioluminescence signal on day 11 (24 hours after the last drug dose administration) and (C) confirms the parasite load on day 11 using qPCR. QD = once daily, QAD = once every 2 days, po=oral drug administration, iv= intravenous drug administration. * = $p > 0.05$.

Figure 4. Anti-leishmanial efficacy of oral DNDI-0690 (50 mg/kg, once daily for 10 days) in a 'New World' CL model (*L. mexicana* M379 REH infection of BALB/c mouse). (A) shows the parasite load, as indicated by *in vivo* imaging of bioluminescent parasites in the infected rump skin over time. (B) shows the bioluminescence signal on day 11 (24 hours after the last drug dose administration) and (C) confirms the parasite load on day 11 using qPCR. QD = once daily, QAD = once every 2 days, po=oral drug administration, iv= intravenous drug administration. * = $p < 0.05$. ** = $p < 0.01$.

514

515 **Figure 5.** Schematic of the experimental set-up of the *in vivo* microdialysis in mice with CL.